

1 TITLE

2 What future for primary aluminium production in a decarbonizing economy?

3 AUTHORS

4 Julien Pedneault, Guillaume Majeau-Bettez, Volker Krey, Manuele Margni

5 ABSTRACT

6 Aluminium is an energy intensive material with an environmental footprint strongly dependent on the
7 electricity mix consumed by the smelting process. This study models prospective environmental impacts
8 of primary aluminium production according to different integrated assessment modeling scenarios
9 building on Shared Socioeconomic Pathways and their climate change mitigation scenarios. Results
10 project a global average carbon intensity ranging between 8.6 and 18.0 kg CO₂ eq/kg in 2100, compared
11 to 18.3 kg CO₂ eq/kg at present, that could be further reduced under mitigation scenarios. Co-benefits
12 with other environmental indicators are observed. Scaling aluminium production impacts to the global
13 demand shows total emission between 1250 and 1590 Gt CO₂ eq for baseline scenarios by 2050 while
14 absolute decoupling is only achievable with stringent climate policy changing drastically the electricity
15 mix. Achieving larger emission reductions will require circular strategies that go beyond primary material
16 production itself and involve other stakeholders along the aluminium value chain.

17 KEYWORDS

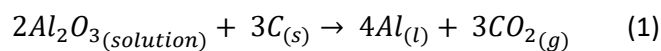
- 18 - Primary aluminium production
- 19 - Carbon footprint
- 20 - Scenario modelling
- 21 - Shared Socioeconomic Pathways
- 22 - Life cycle assessment

23 1 INTRODUCTION

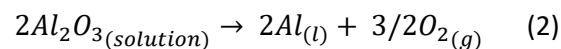
24 Aluminium is the second most used metal in our modern economy, mainly in transportation, packaging,
25 and buildings (Cullen and Allwood, 2013). As the stock per inhabitant keeps growing and shows no sign of
26 saturating yet (Müller, Liu and Bangs, 2013; Maung *et al.*, 2017), the demand for primary aluminium is
27 expected to increase by 34% in the next two decades (IAI, 2020b). Aluminium is an energy-intensive
28 material, with its smelting causing 8% of all worldwide industrial electricity use (Kermeli *et al.*, 2015).

29 Aluminium production starts with the mining of the bauxite ore, followed by its refining with the Bayer
30 process. The resulting aluminium oxide goes through an electrolysis smelting process, the Hall-Heroult
31 process, to produce liquid aluminium, which is finally cast into ingots.

32 The electricity mix consumed by the smelter is the most determinant factor explaining the differences
33 between environmental profiles (Paraskevas, Kellens, *et al.*, 2016; Saevarsdottir, Kvande and Welch,
34 2020). The oxidation of the carbon anode during the Hall-Heroult process is responsible for the other
35 major source of CO₂ emissions, as seen in equation (1).



36 In order to eliminate direct emission of CO₂ and mitigate global warming potential (GWP) (Kovács and
37 Kiss, 2015), a novel reduction technology as equation (2) is developed by aluminium companies, with
38 industrial-scale tests planned or ongoing (Elysis, 2020; RUSAL, 2020):



39 This technology, called inert anode smelting, promises to eliminate all direct CO₂ emissions and to
40 increase productivity (Elysis, 2020).

41 As aluminium is a material with growing demand - especially as a lightweight, corrosive-resistant
42 material in renewable energy infrastructure (Månberger and Stenqvist, 2018) and next generation
43 vehicles (Hatayama *et al.*, 2012) - it is important to anticipate how the carbon intensity of aluminium

44 may evolve in the future. As nations worldwide pledge to decarbonize electricity production as part of
45 decarbonizing their economies, this evolution will in turn influence the desirability (and comparative
46 advantage/disadvantage) of aluminium use within climate change mitigation efforts. An understanding
47 of the evolution of the global greenhouse gas (GHG) emissions of the aluminium industry as a whole is
48 key to inform policy making, as nations ramp up their efforts to mitigate climate change. Even
49 aluminium producers have started declaring their GHG goals for 2030 and 2050 to position their industry
50 in the global climate change mitigation efforts (RUSAL, 2018; Alcoa, 2019; Rio Tinto, 2019) (see SI-1 for
51 specific statements).

52 Research has been done on prospective modelling of the aluminium industry focusing on the question of
53 its recycling and stock dynamics, without directly addressing the long-term influence of the evolution in
54 electricity production mix (Bangs, 2011; Müller, Liu and Bangs, 2013; Bertram *et al.*, 2017). There is a
55 need for an integrated scenario analysis, to expand the scope of analysis beyond the aluminium sector
56 and explore its nexus with the evolving decarbonization of electricity generation.

57 This study aims to align the prospective modelling of environmental impacts of primary aluminium
58 production with the state-of-the-art scenario development paradigms in energy and climate change
59 mitigation analysis, leveraging the different Shared Socioeconomic Pathway narratives (SSPs) (Riahi *et al.*,
60 2017). SSPs describe plausible future challenges for mitigation and adaptation to climate change and serve
61 as foundations to the IPCC Sixth Assessment report, as further detailed in Box 1.

62 We present here an open, top-down modelling framework for the evolution of the carbon intensity of
63 aluminium production and its total carbon footprint. As the projected demand already accounts for the
64 presence of recycling flows (Bertram *et al.*, 2017; IAI, 2020b), and as previous studies extensively
65 describe their stock dynamics (Liu and Müller, 2013; Chen, 2017) and inter-alloy contamination issues
66 (Hatayama *et al.*, 2007; Rombach, Modaresi and Müller, 2012), this article complements existing

67 literature by focusing on primary production and its link with future electricity production and
68 technology developments.

69 It should be recognized that scenarios presented in this study do not have the pretension of predicting
70 the future. Rather, “scenarios are [...] used as scientific tools to explore what futures we could foresee,
71 and which decisions today could most robustly lead to desired outcomes” (Kriegler *et al.*, 2014). By
72 aligning our scenarios with SSP perspective that is articulated in terms of geopolitical, economic and
73 social parameters, the unpredictability is inherent contrary to scenarios based on more physical
74 parameters.

Box 1

SSPs overview

The SSPs are a “scenario framework used by the climate change research community in order to facilitate the integrated analysis of future climate impacts, vulnerabilities, adaptation, and mitigation” (Riahi *et al.*, 2017). The SSPs are based on five narratives describing alternative socio-economic developments and use a set of Integrated Assessment Models (IAMs) to calculate the elaboration of the energy, land-use and the emissions trajectories of SSP-based scenarios (Riahi *et al.*, 2017).

Brief narrative descriptions

SSP1 - Taking the Green road - describes a world “shifting gradually, but pervasively, toward a more sustainable path, emphasizing more inclusive development that respects perceived environmental boundaries” (O’Neill *et al.*, 2017). This implies a reduction of resource and energy intensity. High-income countries support developing countries in their development goals by providing access to human and financial resources and new technologies. This narrative describes a world with low challenges of mitigation and adaptation.

SSP2 - Middle of the road - is an evolution of the societies with no marked shift from historical trends. This narrative describes a world facing moderate challenges to mitigation and adaptation.

SSP3 - A rocky road - is characterized by regional rivalry and international fragmentation. This leads to little international cooperation and low investments in education and in technology for development. Environmental concerns are not prioritized, and consumption remains material intensive, causing high challenges to mitigation and adaptation.

SSP4 - A road divided - represents a world with “highly unequal investments in human capital, combined with increasing disparities in economic opportunity and political power, leading to increasing inequalities and stratification both across and within countries” (O’Neill *et al.*, 2017). Technology development is rapid in high-tech economies while technology diffusion is slow in other regions. SSP4 represents a world with high adaptation challenges combined with low mitigation challenge.

SSP5 - Taking the highway - is “driven by the economic success of industrialized and emerging economies, this world places increasing faith in competitive markets, innovation and participatory societies to produce rapid technological progress and development of human capital as the path to sustainable development” (O’Neill *et al.*, 2017). This techno-optimistic pathway leads to high energy and resource consumption, which in turn results in high challenge in mitigation but low challenge of adaptation.

Mitigation scenarios

Every SSP has a baseline scenario and mitigation scenarios based on the Representative Concentration Pathways (RCPs) (Moss *et al.*, 2010; van Vuuren *et al.*, 2011) representing radiative forcing levels of 1.9, 2.6, 3.4, 4.5 and 6.0 W/m² by 2100. Some combinations of SSPs and RCPs are not possible due to socio-economic conditions. For example, the lowest radiative forcing level that can be reached from SSP3 is 3.4 W/m².

Regional definition

The SSP regional aggregation is made into 5 regions: Asia, Latin America (LAM), Middle East and Africa (MAF), Organisation for Economic Co-operation and Development (OECD) in 1990 and EU member states and candidates, and reforming economies of eastern Europe and the former Soviet Union (REF). See (<https://tntcat.iiasa.ac.at/SspDb/dsd?Action=htmlpage&page=10#regiondefs>) for the exact regional definitions.

76 2 METHODS

77 2.1 PRISMAL FRAMEWORK

78 The PRospective Impacts Scenario for ALuminium (PRISMAL) framework underpins the development and
79 analysis of five internally consistent scenarios for the prospective footprint assessment of primary
80 aluminium production. The open-source Python software (Pedneault and Majeau-Bettez, 2021)
81 integrates life cycle assessment inventories for the entire aluminium production chain and future
82 demand projections (IAI, 2020b) with the SSP narratives (O'Neill *et al.*, 2017). Specifically, PRISMAL
83 articulates distinct scenarios in terms of three key parameters: evolution in electricity mixes, energy
84 intensity reductions of the smelting process and the market penetration of inert anode technology
85 **(Error! Reference source not found.)**. Thus, not only does the framework directly integrate the SSP1-5
86 scenarios and the related mitigation scenarios to determinate the electricity mix of the PRISMAL
87 scenarios, but it also ensures that other factors are modelled consistently with these SSP narratives
88 (O'Neill *et al.*, 2017), as detailed in Table 1 (further descriptions of parameter choices are available in the
89 subsequent methods sections and the SI-2, SI-3 and SI-4). As such, recognizing the mutual influence
90 between industrial and regional energy policies, our top-down model treats the aluminium smelting
91 electricity mix as an integral part of each region's overall electricity mix, experiencing a common
92 decarbonization trend over long-term projections (2050, 2100). The mitigation scenarios considered in
93 this analysis are the one converging to a radiative forcing levels of 1.9 and 2.6 W/m², which correspond
94 to the 1.5°C and 2°C targets articulated in article 2 of the Paris Agreement, respectively (Riahi *et al.*,
95 2017; Rogelj *et al.*, 2018). Results were obtained for all the mitigation scenario available (3.4 , 4.5 and
96 6.0 W/m²) but are not presented and discussed in the article while they are in the range between 2°C
97 and baseline scenarios

98

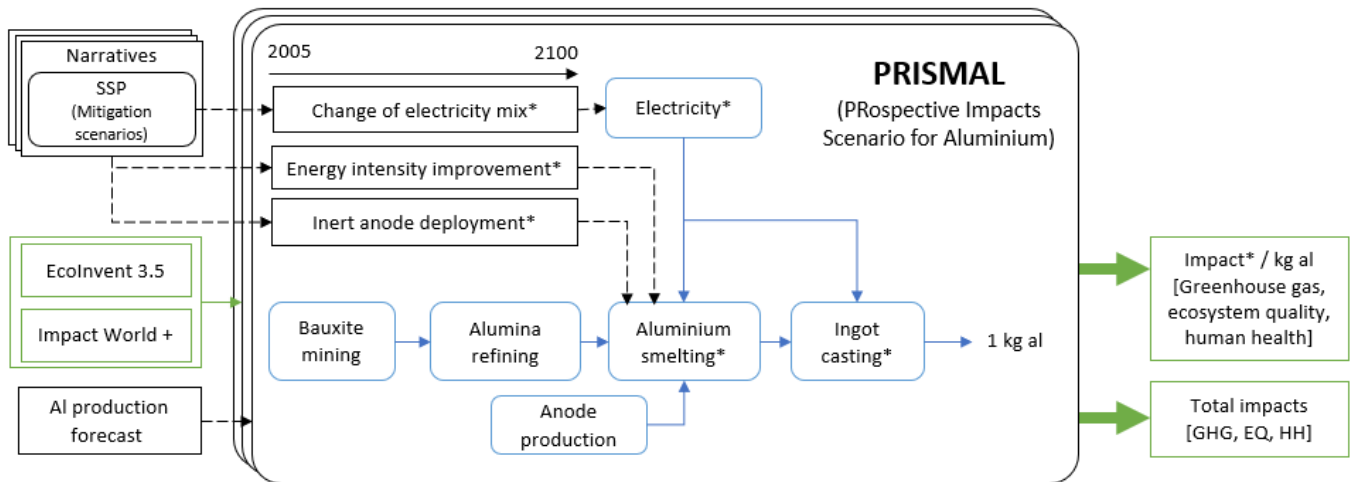


Figure 1: General framework for prospective impacts scenarios modeling aluminium (PRISMAL). Boxes with * indicate that there is a geographical differentiation in the model (Asia, Latin America (LAM), Middle East and Africa (MAF), OECD and reforming economies of eastern Europe and the former Soviet Union (REF). Parameters influencing other life cycle stages such as bauxite mining and refining are assumed constant over time.

Table 1: Qualitative description of different scenarios. Quantitative model and justification are shown in SI. * indicate that there is a geographical differentiation in the model

	Mitigation scenario	Electricity mix trends	Narratives	Smelting energy intensity	Inert anode	
					Deployment speed	Adoption level
PRISMAL1	1.5 °C	SSP1	"Taking the Green road"	Low	Quick	100%
	2.0°C					
	Baseline					
PRISMAL2	1.5 °C	SSP2	"Middle of the road"	Medium	Slow	75%
	2.0°C					
	Baseline					
PRISMAL3	1.5 °C	Not applicable				
	2.0°C	Not applicable				
	Baseline	SSP3	"A rocky road"	High	None	0%
PRISMAL4	1.5 °C	Not applicable				
	2.0°C	SSP4	"A road divided"	Medium*	Slow	75%*
	Baseline					
PRISMAL5	1.5 °C	SSP5	"Taking the highway"	Medium	Quick	100%
	2.0°C					
	Baseline					

100

101

102

103

104 2.2 SPACE AND TIME RESOLUTION

105 PRISMAL distinguishes between five different regions, identical to SSP framework (see box 1). A global
106 aggregation is performed to obtain a global average based on the market share of aluminium production
107 by region (Riahi *et al.*, 2017). We used historical data (IAI, 2020c) for 2005 and 2010 assessments, while
108 2019 market share (IAI, 2020c) has been used as a proxy for 2020. For subsequent years, constant
109 market share based on 2019 data was assumed. A sensitivity analysis has been performed to test this
110 latter assumption. As time resolution, PRISMAL covers a period from 2005 to 2100 with decennial
111 resolution from starting at 2010.

112 2.3 DECARBONIZATION OF ELECTRICITY MIX

113 The electricity mix of aluminium smelters often differs significantly from that of their region (Koch and
114 Harnisch, 2002). Consequently, the PRISMAL framework could not directly employ the regional
115 electricity mixes forecasted by the different SSPs. Rather, the PRISMAL framework extracts the *trends* of
116 these projected regional electricity mixes, and it uses these trends to update the smelter mixes. For
117 example, if in a given scenario the market share of coal is projected to decrease by 65% between 2020
118 and 2030 in the electricity mix of Asia, then a similar percentage reduction is applied to the share of coal
119 in smelter mix of that region.

120 We first compile the most recent aluminium smelter consumption mix (z_i^t , for i element of coal, hydro,
121 etc.), along with historical mixes (2005, 2010) from IAI data (2020e). The 2019 data were used for 2020
122 since they were not available yet. In order to aggregate the different IAI regions into 5 regions, we
123 calculated the weight average of electricity mix of North America, Europe and Oceania to have the
124 electricity mix of OECD; Africa and Gulf and Middle East region for MAF region; China and “Asia except
125 China” for Asia; and we supposed an equivalent European electricity mix for REF. No aggregation was
126 needed for South America.

127 The future electricity mix trends from 2020 to 2100 for each of the 5 regions were extracted from SSP
 128 results (Bauer *et al.*, 2017; Riahi *et al.*, 2017) using their respective marker scenario. A marker scenario is
 129 the interpretation of one SSP by one specific selected IAM model (SSP1 – IMAGE, SSP2 – MESSAGE-
 130 GLOBIOM, SSP3 - AIM/CGE, SSP4 – GCAM4, SSP5 - REMIND-MAGPIE) (Riahi *et al.*, 2017). From the
 131 market share of each technology i at each time t (s_i^t) we calculate the positive (d_i^{t+}) and negative (d_i^{t-})
 132 variations, following equations (3) and (4), respectively.

$$d_i^{t+} = \begin{cases} s_i^{t=1} - s_i^{t=0} & \text{if } s_i^{t=1} - s_i^{t=0} > 0 \\ 0 & \text{otherwise} \end{cases} \quad (3)$$

$$d_i^{t-} = \begin{cases} s_i^{t=1} - s_i^{t=0} & \text{if } s_i^{t=1} - s_i^{t=0} < 0 \\ 0 & \text{otherwise} \end{cases} \quad (4)$$

133 The decreases are then normalised by their initial market share, forming a relative decrease coefficient
 134 Δ_i^{t-} (equation (5)). The increases are also normalised Δ_i^{t+} , but relative to the sum of all the increased
 135 (equation (6)), capturing each technology's relative share of new production capacity.

$$\Delta_i^{t-} = \begin{cases} \frac{d_i^-}{s_i^{t=0}} & \text{if } s_i^{t=1} \neq 0 \\ 0 & \text{otherwise} \end{cases} \quad (5)$$

$$\Delta_i^{t+} = \frac{d_i^+}{\sum_j d_j^+} \quad \forall i \quad (6)$$

136 These decreasing and increasing trends in the regional market shares of each technology are then
 137 applied to update the smelter mix. A vector $x_i^{t=1}$ containing the negative variation of the smelter
 138 market share is created with the product of smelter market share of aluminium smelter ($z_i^{t=0}$) and the
 139 normalised trends (Δ_i^{t-}) as in equation (7). The vector with the positive variation ($y_i^{t=1}$), which displace
 140 the technologies that lost market shares in x , is calculated from the product of the sum of the negative
 141 vector (x) and the normalised increases (Δ_i^{t+}) as in equation (8). Finally, the new market share of
 142 aluminium smelter $z_i^{t=1}$ is obtained by adding market share at previous time period and the positive and

143 the negative variations. This calculation is repeated for every region and every time step between 2030
 144 and 2100.

$$x_i^{t=1} = z_i^{t=0} * \Delta_i^- \quad \forall i \quad (7)$$

$$y_i^{t=1} = \left(- \sum_j x_j^{t=1} \right) * \Delta_i^+ \quad \forall i \quad (8)$$

$$z_i^{t=1} = z_i^{t=0} - x_i^{t=1} + y_i^{t=1} \quad (9)$$

145 An example of calculation and a comparison of the evolution of the calculated electricity mixes for
 146 PRISMAL scenarios and SSP electricity mixes is presented in SI-2. Environmental data and impact
 147 calculation are explained in section 2.6.

148 2.4 IMPROVEMENT OF THE ENERGY INTENSITY OF THE SMELTING PROCESS

149 Based on the conservation of energy law and thermodynamic calculations, the theoretical minimum
 150 energy requirement for the electrolysis process is 6.23 kWh/kg of aluminium (Obaidat *et al.*, 2018) while
 151 the world average in 2018 was 14.2 kWh/kg (IAI, 2020d). Part of the excess energy goes into a necessary
 152 heat loss to maintain the right amount of frozen electrolyte protecting the cell lining, and the rest is
 153 consumed to overcome resistance of the cell components (Obaidat *et al.*, 2018).

154 We formulated a techno-pessimistic, techno-optimistic, and middle-of-the-road scenario for the energy
 155 efficiency of smelting over time to account for technology evolution pathways that are consistent with
 156 the various SSPs. With current best practice, an energy intensity of 12.3 kWh/kg can be achieved (Hydro,
 157 2020). In our most techno-pessimistic scenario, no further improvement is technically possible, and all
 158 efficiency gains come from a broader adoption of these currently known best practices across the entire
 159 industry by 2100. In this worst-case scenario, we therefore model a linear progression from the current
 160 average efficiency to 12.3 kWh/kg worldwide by 2100.

161 Ongoing research could pave the way to going beyond current practice by using Cu-inserted collector
162 bar, developing wettable cathodes made of or coated with TiB₂ (Li *et al.*, 2008; Heidari, 2012),
163 minimizing the distance between the anode and the cathode (Haraldsson and Johansson, 2018),
164 designing slotted or perforated anodes to reduce bubble thickness under the anode (Tian *et al.*, 2013)
165 and improving the overall operation of electrolysis cells with industry 4.0 technologies by optimising
166 operation of the smelter due to the use of historical and real-time data, digital model and machine
167 learning (Haraldsson and Johansson, 2018; Gupta and Basu, 2019).
168 Consequently, our techno-optimist scenario extrapolates historical trends in energy efficiency gains, as
169 per equation (3),

$$\frac{a}{(t - h)} + 6.23 = \text{Energy intensity} \quad (10)$$

170 where t represents the year, 6.23 is the minimum thermodynamic limit in kWh/kg Al. Fitting constants
171 were determined by regression via the sum of least squares, giving an a = 1177 and h = 1862. The
172 regression used historical data from 1890 to 1970 from McGeer et al.(1986) and from IAI for the period
173 between 1980 and 2015 (IAI, 2020d). The extrapolation, with a R² of 0.992, leads to an average global
174 smelting energy intensity of 12.5 kWh/kg of primary aluminium by 2050, and 11.2 kwh/kg by 2100 what
175 we, and experts from the industry informally consulted, judge ambitious but achievable. The average of
176 those two scenarios is then calculated to obtain an intermediate evolution pathway in smelting energy
177 intensity.

178 For each PRISMAL scenario, we assigned a level of energy intensity (low, medium, or high) based on the
179 SSP narratives to ensure consistency within each scenario. Consequently, the PRISMAL1 scenario is the
180 least energy intensive because of the willingness to decrease global energy consumption inherent of the
181 associated narrative. The energy intensity in the PRISMAL2 scenario is at a medium level, while
182 PRISMAL3 and PRISMAL5 follow the upper threshold of energy intensity as neither of the associated

183 narratives describe any willingness to improve energy use. The energy intensity of PRISMAL4 depends
184 on the region; where OECD follows the lower limit, MAF the upper and LAM, Asia and REF the
185 intermediate level of energy intensity. A graphical representation of the described extrapolations and
186 numerical values for the energy intensities are available in SI-3.

187 2.5 INERT ANODE DEPLOYMENT

188 The deployment of the inert anode smelting technology depends on its competitiveness relative to
189 current technology. Replacing carbon anode with an inert anode would eradicate the direct emissions of
190 CO, CO₂, SO₂, fluorocarbon (PFC) and polycyclic aromatic hydrocarbon (PAH) generated by the
191 traditional Hall-Heroult process (Andrey S., Sai Krishna and Peter V., 2018)

192 To model the deployment over time, a logistic curve has been used starting from 2020 (Foster, 1986).

193 The market share of inert anode smelting technology over time ($D_{in,t}$) is described by equation (11)

$$D_{in,t} = \frac{A}{1 + e^{-k * (t-t_h)}} \quad (11)$$

194 where A is the total amplitude possible of deployment over the examined time period (between 0 and
195 1); k is the steepness of the curve, and t_h is the year of the middle of the curve where the technology
196 penetrated 50% of the market. We defined A , t_h , and k consistently with the five narratives to control
197 the deployment the technologies for each PRISMAL scenario (see Table 1).

198 Narratives for SSP1 leads to “a rapid technological change is directed toward environmentally friendly
199 processes” (O’Neill *et al.*, 2017). As inert anode development is driven by environmental considerations,
200 we assumed a complete adoption over the century with a quick level of adoption from 2050. For
201 PRISMAL2, an assumption of slow penetration rate and a maximum amplitude of 75% is made. For
202 PRISMAL3, we assumed no deployment of inert anode technology because the narrative describes a
203 world with a very slow technological development and no focus on clean technology. PRISMAL4 is split

204 into three levels due to the assumed socioeconomic inequalities between regions. Deployment in OECD
205 is slow but complete by the end of the century due to the wealth of the region. Asia, LAM and REF, the
206 regions with an intermediate GDP also deploy the technology with a slow rate and a maximum
207 amplitude of 75% but start after OECD. Finally, in MAF, the region with the lowest GDP, the adoption is
208 also slow and delayed but the maximum amplitude is only 50%. For PRISMAL5, the relevant narrative
209 states that “technological innovation is very high, with a focus on increasing labor productivity, fossil
210 energy supply, and managing the natural environment” (O’Neill *et al.*, 2017). Because inert anode is
211 considered as a green technology, the deployment is assumed quick and the amplitude is total, but it
212 starts later than the one in PRISMAL1, as this techno-optimistic narrative does not adopt green
213 technology in the first half of the century. The graphical evolution of the parameters with the numerical
214 parameter values are shown in SI-4.

215 2.6 ENVIRONMENTAL IMPACTS

216 To assess environmental impact profiles of the five PRISMAL scenarios, a link between our modelling
217 parameters and environmental impacts must be made. Life cycle inventory data related to the supply of
218 material and energy flows are calculated with unit processes from *ecoinvent* (version 3.5, cut-off)
219 (Wernet *et al.*, 2016). The environmental impacts potentially caused by these emissions and resource
220 extractions were estimated with the IMPACTWorld+ life cycle impact assessment method (Bulle *et al.*,
221 2019) supported by the SimaPro v8.5.2.2 software. We generated an impact profile with three endpoint
222 indicators: climate change (CC) [kg CO₂ eq], human health (HH) measured in disability-adjusted life years
223 [DALY] and ecosystem quality (EQ) measured in potentially disappeared fraction of species over a square
224 meter and during a year [PDF.m².yr]. The two latter indicators represent aggregated damage level
225 indicators building on natural science modeling (Verones *et al.*, 2017). To avoid double counting and
226 focusing on CC indicator, we removed CC midpoint indicator from HH and EQ endpoint indicators. HH

227 takes into account ozone layer depletion, human toxicity cancer, human toxicity non-cancer, particulate
228 matter formation, photochemical oxidant formation, ionizing radiations and water availability. The EQ
229 includes marine acidification, freshwater acidification, terrestrial acidification, freshwater
230 eutrophication, marine eutrophication, freshwater ecotoxicity, ionizing radiations, water availability,
231 land transformation and land occupation. Only the short-term damage level indicators (i.e., within a
232 time horizon of 100 years) have been included.

233 2.6.1 Impacts of electricity mix

234 The environmental profile of the electricity mix is calculated from the market share of each energy
235 technology (biomass, coal, gas, hydro, nuclear, oil, solar and wind). The environmental profile of each
236 electricity technology has been calculated by doing a weight average of the impact of different
237 processes and region using production volume ofecoinvent. For example, for hydroelectricity, we
238 calculated the CC, EQ, and HH per kWh of different technologies: reservoir non-alpine region, reservoir
239 alpine region and run-of-river for different geography available on ecoinvent. A weight average based on
240 the volume of all those technologies and geography is then made to have an average impact of hydro
241 production.

242 As *ecoinvent* does not include carbon capture and sequestration (CCS) technologies, a reduction factor
243 on GHG impact was used for these technologies in the electricity mixes. These factors were calculated as
244 the ratio of median value for the life cycle carbon intensity of different electricity generation
245 technologies with and without CCS as published in the IPCC Fifth Assessment Report on mitigation of
246 climate change (Edenhofer *et al.*, 2014). The factor used for coal CCS is 27% and 35% for gas meaning
247 that CC emissions are 27% and 35% of the original impact. No factor was applied on EQ and HH
248 indicators. For the biomass CCS we directly apply the value of -0.776 kg CO₂ eq/kWh (Edenhofer *et al.*,
249 2014) and did not change the EQ and HH indicators either.

250 Tables with calculated values of CC impact per kWh for PRISMAL, mitigation scenarios and regions are
251 available in SI-5.

252 2.6.2 Inert anode smelting modeling

253 Inert anode is a technology still in development for an industrial scale. Data is lacking and exact
254 composition of the inert anode material is still confidential. Therefore, a screening LCA of inert anode
255 technology has been made based on Lovács & Kiss (2015). We assumed an anode composition of 55%
256 copper, 20% nickel and 25% of iron. We also assumed that the inert anode will have a lifetime thirty
257 times longer than that of a prebaked anode (ELYSIS, 2019).

258 To model the smelting process with inert anode, we adapted the smelting process (Aluminium, primary,
259 liquid {RoW}) aluminium production, primary, liquid, prebake) by removing direct emissions of CO, CO₂,
260 SO₂, PFC and PAH. Emissions of HF (g) has been maintained because the fluoride-containing electrolyte
261 will still generate those gases (Kovács and Kiss, 2015). *Ecoinvent* data (Wernet *et al.*, 2016) and
262 calculated impacts of the technology are available at SI-6.

263 One of the biggest uncertainties concerning the inert anode smelting technology lies in the process
264 energy consumption. The total theoretical energy requirement for the inert anode reaction is 9.184
265 kWh/kg of Al in comparison to 6.23 kWh/kg of Al for the traditional Hall-Heroult process (Obaidat *et al.*,
266 2018). The cost of electricity currently contributes 35% of the total cost of smelting (Allwood and Cullen,
267 2012); a technology with a higher energy intensity would not be economically viable for smelters. For
268 that reason, we assumed an equal energy intensity for both the Hall-Heroult and inert anode process
269 over the years. However, policy can also drive the deployment of the inert anode technology, even
270 when it's not economically competitive with a carbon anode, which means that an adoption of the
271 technology could be done with a higher electricity consumption. To evaluate the consequence of such a
272 context, a sensitivity analysis is done with an extra consumption of 3 kWh/kg for the inert anode which

273 is the difference between the theoretical minimal energy requirement of the two reduction
274 technologies.

275 2.6.3 Unit process

276 The cradle-to-gate or gate-to-gate impact profile of each process used by PRISMAL is pre-calculated with
277 the Simapro life cycle assessment software. In order to get a single value impact, despite country-level
278 specificity from ecoinvent, we take a weighted average of the member countries using the regional
279 production volumes provided in ecoinvent. From the precalculated processes, we removed the physical
280 input flows already accounted for in the PRISMAL model to avoid double counting. For example, the
281 impact profile of the alumina production process does not account for impacts from bauxite mining.
282 Similarly, the impact profile of the smelting process with a prebaked anode does not account for the
283 impacts of the anode, the alumina and the electricity production supplying the process. Weighted
284 averaged impact profiles of all the processes used for calculation in the PRISMAL model are available in
285 SI-7. Those precalculated environmental data are used as an input of the PRISMAL program.

286 From the precalculated impacts, PRISMAL uses a technological matrix (with dimension 7 x 7 processes,
287 see SI-8) to calculate the amount of each process needed to produce 1 kg of primary aluminium ingot.
288 The electricity mix used for smelting and casting of liquid aluminium at the smelter is the same as these
289 two processes always occur at the same location.

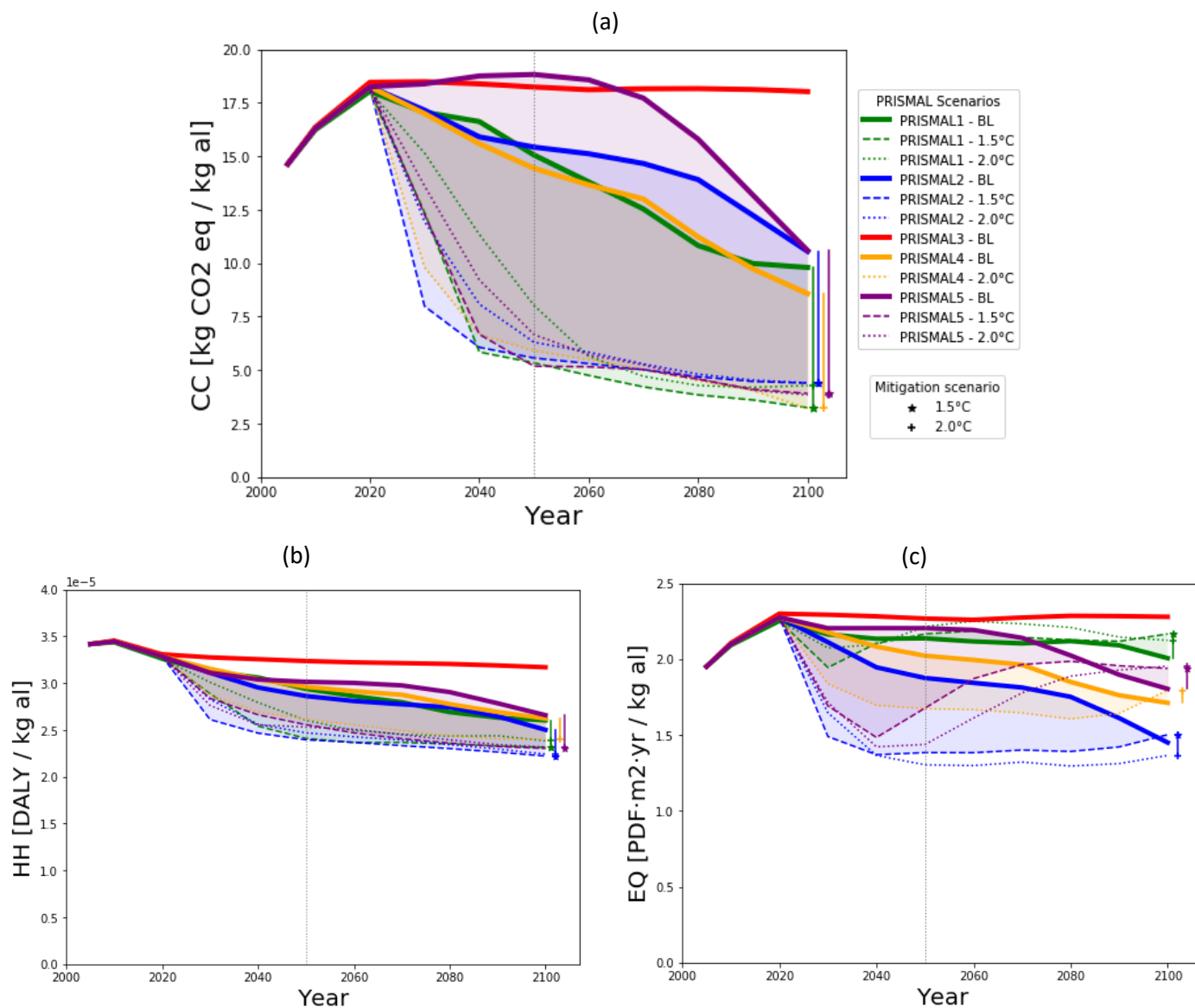
290 2.7 MAGNITUDE OF FUTURE PRODUCTION

291 The absolute environmental impacts of primary aluminium production are calculated by scaling the
292 impact intensity to the global production of primary aluminium. The production volumes to 2050 were
293 obtained from the IAI global alucycle (IAI, 2020a) based on a dynamic material flow model (Bertram *et*
294 *al.*, 2017) according to their moderate Covid-19 demand impact scenario.

295 **3 RESULTS**

296 **3.1 PROSPECTIVE ENVIRONMENTAL IMPACTS**

297 The evolution of the environmental intensity indicators for global primary aluminium production
 298 depends on the PRISMAL scenarios and their associated mitigation scenarios (Figure 2). Results of all
 299 PRISMAL runs are available [here](#).



300 *Figure 2: Average global GHG (a), HH (b) and EQ (c) impact per kilogram of primary aluminium for different PRISMAL scenarios.*
 301 *The dashed lines of every PRISMAL scenario represents the result with the electricity mix of the lowest mitigation scenarios*
 302 *possible with the associated SSP and the colored area represent the range between the baseline and the lowest mitigation*
 303 *scenario. Numerical values for the three indicators are presented in SI-9.1, SI-9.2 and SI-9.3.*

304 Looking first at the baseline scenario mitigation, PRISMAL scenarios 1, 2 and 4 show a steady decrease in
305 GHG emission intensity of aluminium production from 2020 to 2050, mainly due to reduced emissions
306 intensity of electricity generation of the underlying SSP and the improvement of energy intensity of the
307 smelting process. PRISMAL scenarios 3 and 5 show no emissions reductions to 2050 as a result of
308 persistent high emissions intensity of electricity generation from SSPs 3 and 5 due to the increased
309 challenges to mitigation in these narratives (see Box 1). In 2050, a decrease of 20% from 2020 level is
310 expected for the best-case scenarios and more than 50% in 2100. Numerical values are available in SI-
311 9.1, SI-9.2 and SI-9.3.

312 With the integration of the SSP mitigation scenarios in our analysis, a more drastic and rapid reduction
313 of carbon intensity is observed. Naturally, the carbon intensity declines fastest in the 1.5°C (1.9 W/m²)
314 scenarios. However, with the exception of PRISMAL 3 scenario, in the long-term, the emission intensity
315 of aluminium production converges to approximately the same levels under the 1.5 and 2.0°C targets,
316 respectively (Figure 2 (a)). The Human health (HH) (Figure 2 (b)) indicator follows similar trends, thus
317 showing an environmental co-benefits of low-carbon system (Hertwich *et al.*, 2015; Gibon, Arvesen and
318 Hertwich, 2017).

319 For the HH indicator, all PRISMAL scenarios decrease in the future except PRISMAL3. Alumina refining is
320 the main contributor of total HH impacts (due to chromium and arsenic emissions to water) followed by
321 the electricity used (with the related emissions of SO₂, NO_x and PM from fossil-fuelled electricity plants).

322 For the EQ indicator, PRISMAL2 represents the scenario with the lowest EQ impacts. Surprisingly,
323 PRISMAL1 and scenarios with high mitigation do not display the lowest impact because of the larger
324 market share of photovoltaic and biomass electricity. Those two technologies have a potentially higher
325 impact on land transformation in comparison to other electricity technologies, increasing the EQ
326 endpoint impacts indicator. The increased of EQ impacts observed in the mitigation scenario of
327 PRISMAL1 , PRISMAL2 , PRISMAL4 and PRISMAL5 is due to a net increase in market share of photovoltaic

328 and biomass. This potential trade-off between climate change and ecosystem quality indicators should
329 be further studied.

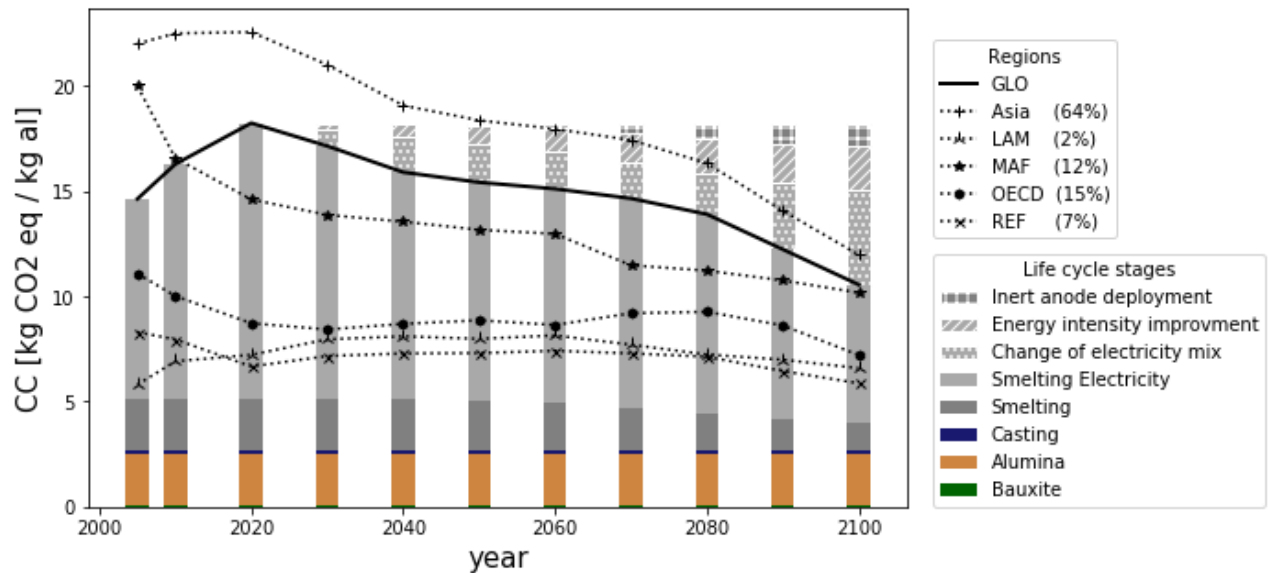
330 With a focus on the PRISMAL2 scenario, Figure 3 shows a contribution analysis to GHG emissions of the
331 global primary aluminium production (GLO) as well as the regional developments for five regions for the
332 baseline. Similar graphics with 1.5°C target and 2.0°C target scenarios are available in SI-10. The role of
333 three key factors in mitigation is depicted: (i) the change of electricity mix, (ii) the improvement of
334 energy intensity of the smelting process and (iii) the progressive deployment of inert anode. The
335 contribution of the improved energy intensity is obtained by the product between the impact of
336 electricity set at the year 2020 (kg CO₂ eq/kWh) and the variation of energy intensity between two
337 future periods of time (kWh/kg al). The improvement related to the changes of electricity mix is
338 calculated as the variation of impact between the electricity mix between two time periods (kg CO₂
339 eq/kWh) multiplied by the electricity intensity of 2020. The improvement of inert anode deployment is
340 the difference between the impact of prebaked anode and inert anode (direct emission and anode
341 production). Emissions related to alumina refining and bauxite mining remain constant as assumed by
342 our scenario evaluation.

343

344

345

346



347

348 *Figure 3: Contribution analysis of global (GLO) primary aluminium production for PRISMAL2 and evolution of carbon intensity*
 349 *per region with the baseline scenario. Hall-Heroult process and its direct emissions is grouped with the anode production into*
 350 *the smelting stage. The contribution analysis from life cycle stages is made for the GLO region. The percentage in parenthesis*
 351 *in the region's legend entry represents the market share of each regions used from 2020 to 2100.*

352 The decarbonisation of the electricity mix has the biggest potential for reducing carbon intensity of
 353 aluminium production because of the wide range in carbon intensity within electricity production
 354 technologies. The gains are even higher and quicker with the 1.5°C and 2.0 °C mitigation scenarios. The
 355 improvement of operation of smelting plant to reduce the energy intensity of the electrolysis can also
 356 contribute to the overall reduction of the industry. Inert anode can reduce the carbon footprint of
 357 aluminium production up to 10% because direct emissions are not a major contributor of overall GHG
 358 emissions. However, with rapid decarbonization of electricity generation under the 1.5 and 2.0°C
 359 scenarios, smelting emissions and emissions from alumina production become a substantial share of
 360 remaining emissions, emphasizing the need to reduce those emissions as well. Under our default
 361 assumptions (copper-nickel-iron anode with a 30 times longer lifetime - see section 2.6.2 and SI-6 for
 362 more information), the environmental gains related to inert anode deployment would only become
 363 substantial after 2050. As shown by the sensitivity analysis (SI-11), a rebound effect could be observed if
 364 the energy intensity of the inert anode is 3 kWh/kg higher than the one of the Hall-Heroult process

365 assumed in our baseline scenario and if the electricity mix supply has a high carbon intensity. For the
366 mitigation scenarios with a low carbon electricity mix, no rebound effect is observed and inert anode
367 technology lead to environmental gains even with an extra electricity consumption.

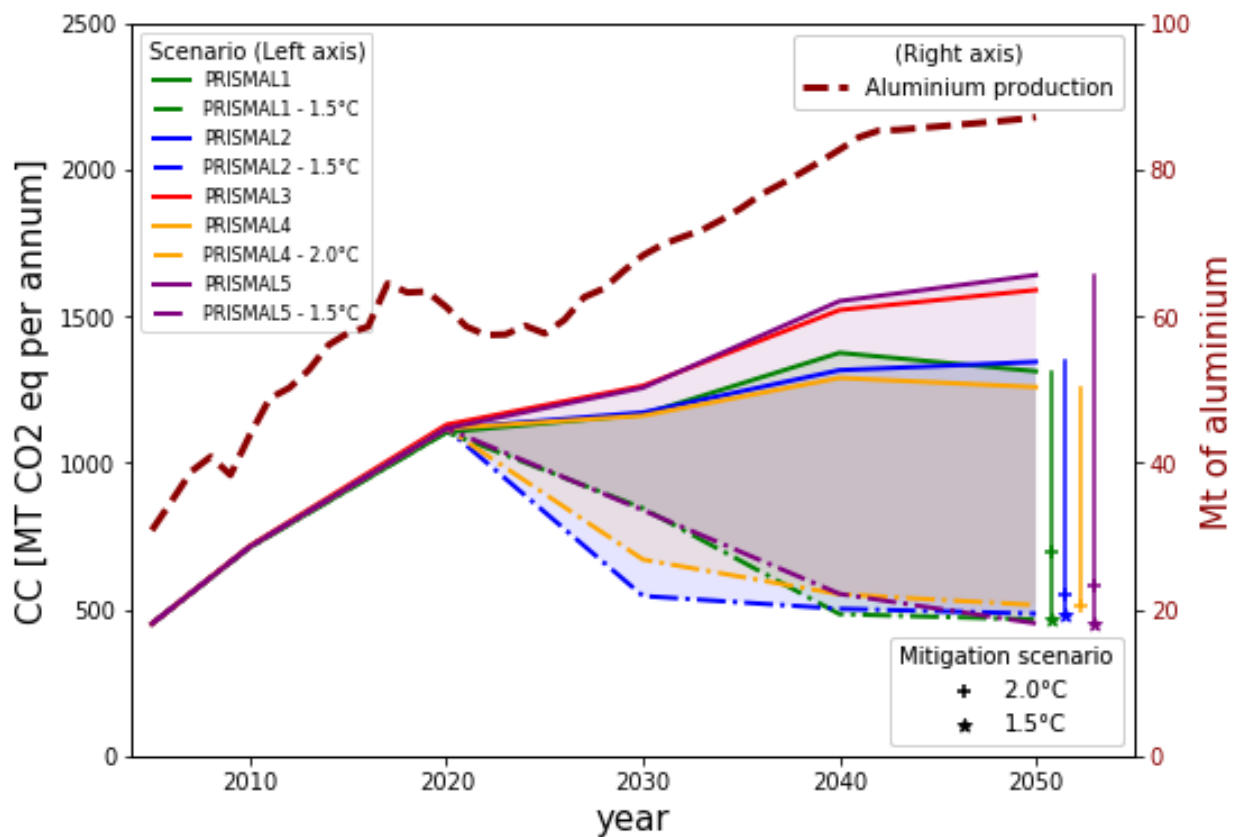
368 The prospective GHG intensity over time is also provided for five regions of the globe, with Asia
369 currently having the highest market share (64%) and also showing largest improvement potential to
370 2050, mainly due to the decarbonization potential of a still heavily fossil-based electricity mix. A
371 convergence across regions is observed. The other PRISMAL scenarios follow similar trends, though with
372 a lesser degree of convergence, except PRISMAL3, which, in accordance with the SSP3 narrative, shows
373 almost no regional convergence at all (see SI-12).

374 The expected convergence ensures that uncertainties of future regional market shares do not heavily
375 influence our future weighted global average. The consideration of SSP mitigation scenarios emphasize
376 this convergence because the electricity mix becomes more uniform in order to achieve a specific
377 radiative forcing level. Moreover, a sensitivity analysis on different geographical allocation comparing
378 extreme and conservative schemes for new future aluminium production capacity shows no major
379 changes in global results because of this convergence of electricity mix and limited addition of new
380 capacity in comparison of already existing infrastructure (see SI-13).

381 3.2 TOTAL PRODUCTION

382 A scaling of the impact intensity results for total primary aluminium production projection (Bertram *et*
383 *al.*, 2017; IAI, 2020b) has been made in order to quantify absolute impacts of industry as a whole. Figure
384 4 shows total GHG emissions of the aluminium production worldwide according to each scenario to
385 2050 and the underlying annual aluminium production (See SI-14 for values). By looking at the baseline
386 scenarios, we observe that the improved impact intensity of aluminium production is not sufficient to
387 offset the increase in production volume. According to the model, the total impact of the aluminium

388 industry will increase between 18% (PRISMAL1) and 40% (PRISMAL3) from 2020 to 2050, while the
 389 production increases by 42% during the same period. A relative decoupling is observed for PRISMAL1,
 390 PRISMAL2 and PRISMAL4 meaning that the production growth rate is higher than pollution growth rate.
 391 The objective of absolute decoupling, a net stabilisation or reduction of impacts with a concurrent
 392 increase in production, is not reached. Thus, the absolute decoupling from 2020 levels could be
 393 observed with 1.5 and 2.0°C mitigation scenarios as shown by the blue area and the vertical lines of each
 394 PRISMAL scenarios.



395

396 *Figure 4: Total GHG emissions of the aluminium production according different PRISMAL scenarios and annual production of*
 397 *primary aluminium. The blue area represents the range between the baseline mitigation scenario and the 1.5°C mitigation*
 398 *scenario of PRISMAL2. The vertical lines represent the range between baseline scenario and lower possible mitigation*
 399 *results.*

400 4 DISCUSSION

401 4.1 STRATEGIC IMPLICATION

402 Globally, the different PRISMAL scenario runs demonstrate that major improvements in the carbon
403 intensity of aluminium can realistically be achieved before 2050, and even more so extending toward
404 2100. These improvements, however, mostly depend on aggressive climate mitigation policies that extend
405 beyond the aluminium sector and into the decarbonization of electricity production chains. Thus, the
406 different mitigation scenarios robustly converge to reductions of 55-70% from 2020 level in 2050 and to
407 reductions between 75 and 80% in 2100. When taking the projected increase of aluminium production,
408 the PRISMAL2 scenario with 1.5°C policies (RCP 1.9) shows a reduction of 632 Mt of CO₂ eq compared to
409 the baseline of 1117 Mt of CO₂ eq in 2050.

410 This unusual importance of electricity in the aluminium production chain hints at a strategically significant
411 virtuous cycle: just as aluminium is expected to play a major role in climate mitigation efforts (renewable
412 energy infrastructure with battery production (Månberger and Stenqvist, 2018) and mounting structures
413 and frames for photovoltaic panels (Maurice Bödeker and Bauer Martin Pehnt Heidelberg, 2010),
414 lightweighting of transport (Bertram, Buxmann and Furrer, 2009), etc.), these mitigation efforts are
415 expected to play a major role in the reduction of this metal's environmental and carbon footprint.

416 Consequently, when prospectively assessing the future environmental impacts of green technologies, the
417 aluminium contribution to their lifecycle impact is likely to be disproportionately overestimated if current
418 aluminium production data is employed, as any scenario that involves a massive use of these green
419 technologies likely also involves a particularly important decarbonization of the aluminium value chains.

420 As our projections show, the future decarbonization of aluminium production depends mostly on a factor
421 that is not within the direct control of the industry actors: the availability of affordable and reliable low-

422 carbon electricity sources. Decarbonized energy sources either grow increasingly constrained (limited
423 hydropower potential, land use competition for bioenergy (Chen and Önal, 2016; Ryberg, Robinius and
424 Stolten, 2018), material constraints (Moreau, Dos Reis and Vuille, 2019)) or require buffer capacity,
425 integrated grid networks (Worighi *et al.*, 2019), or extensive sequestration activities (Bui *et al.*, 2018) in
426 order to perform. These constraints and extensive value chains lead to the involvement of multiple actors,
427 even in the case of vertically integrated energy production. A system's perspective and coordinated efforts
428 will therefore be required for aluminium to serve as a strategic material in the global climate mitigation
429 efforts.

430 The aluminium industry has a more direct influence on the other two parameters of this study: gains in
431 energy efficiency and deployment of inert anodes. Though of lesser relative importance than the
432 decarbonization of the electricity mix, efforts to increase energy efficiency are nonetheless expected to
433 lead to major cumulative environmental impact reductions (between 48 and 135 Mt CO₂ eq by 2050),
434 especially since cost reductions through efficiency gains will likely stimulate these efforts.

435 Conversely, the short-term cost effectiveness and feasibility of inert anode technology remains to be
436 demonstrated. It is unclear whether it would prove feasible to retrofit existing installations. Our scenarios
437 present a level of technological penetration that is limited by technological readiness and the stock
438 turnover of aluminium smelters, and consequently we anticipate substantial industry-wide
439 decarbonization benefits from inert anodes only after 2050. Inert anodes can thus be seen as a long-term
440 strategic investment, especially if the more aggressive electricity decarbonization scenarios come to pass
441 and direct smelting emissions represent a more important share of the total lifecycle impacts (e.g., direct
442 emissions representing 25% of emissions by 2050 in the PRISMAL2 scenario with 2.0°C policies without
443 inert anodes). As any new technology, a life-cycle perspective should be taken as more data on inert anode
444 production and use become available, in order to avoid burden shifts and unintended consequences.

445 According to baseline scenarios, we can expect a relative decoupling between environmental impacts and
446 primary aluminium production for baseline scenarios in the next three decades, except for PRISMAL 3 and
447 PRISMAL5 scenarios which are based on a narrative with high social-economic challenges for mitigation.
448 While aluminium producers have started to set environmental goals for the next decades (see SI-1), our
449 analysis shows that an absolute reduction of emissions by 2050 for this sector would require a drastic
450 change in electricity mix consistent with an aggressive climate change mitigation policy. Carbon capture
451 would still be necessary in the most optimistic scenarios to capture the remaining emission of 500 Mt CO₂
452 eq per annum.

453 Beyond improving the environmental intensity of primary production, which has been the focus of this
454 analysis, reduction of the overall material demand can contribute to the achievement of a low carbon
455 economy (Material Economics, 2016) and an absolute decoupling of the aluminium sector. This could be
456 achieved by the adoption of circular economy strategies that go beyond primary material production
457 itself and involve other stakeholders along the aluminium value chain, namely: bauxite mining, alumina
458 refining, material recirculation, product material efficiency and circular business models (Material
459 Economics, 2016). Such circular economy strategies seem necessary to overcome alloy
460 intercontamination issues in recycling (Rombach, Modaresi and Müller, 2012) and to reduce of
461 transformation and fabrication losses (Cullen and Allwood, 2013). In a report made by Material
462 Economics (2016) on potential future gains of circular economy, a possible CO₂ emission reduction of
463 300 Mt (-24% in comparison of their baseline scenario) by 2050 was calculated considering different
464 circular initiatives within the aluminium sector.

465 Material substitution strategies can further contribute to GHG mitigation potential. Aluminium can
466 displace other materials with overall life cycle benefits in respect to the targeted function achieving
467 reduction that are not taken into account here and would compensate some of the emissions reductions

468 potentials as shown in Figure 4. For instance, substituting steel by aluminium reduces use-phase
469 emissions due to light-weighting (Bertram, Buxmann and Furrer, 2009).

470 While the mentioned circular economy and substitution strategies were not assessed by the present
471 study, they should be considered as a means to reach absolute decoupling and meet more ambitious
472 net-zero targets for the 2050 time horizon or beyond and thus mitigate reputational risks of the
473 aluminium industry and help nations to achieve their pledges in international climate agreements.

474 4.2 VALIDATION AND LIMITATIONS

475 The global and regionalized lifecycle GHG relative impacts of PRISMAL are within ranges of previous
476 studies (McMillan and Keoleian, 2009; Paraskevas, Van de Voorde, *et al.*, 2016), as further discussed and
477 illustrated in SI-15. The scaled-up global emissions slightly exceed the 1 billion tons of CO₂ eq of GHG
478 emissions estimated by the IAI in 2018 for the whole industry (Vatne, 2019).

479 Our prospective scenario analysis focuses on the evolution of the electrolysis process, which accounts
480 for 70% of the cradle-to-gate GHG emissions of primary aluminium production. Since bauxite and
481 alumina refining contribute less than 30% GHG impact for all baseline scenarios, this focus is not
482 expected to alter our conclusions. Nevertheless, further research could explore impact reduction
483 potential in both of these upstream life cycle stages.

484 While we did not specifically analyse the impact evolution of the alumina refining, few elements
485 deserved to be discussed. Almost 60% of the CC impact of alumina refining comes from the heat
486 consumed by the process (Nunez and Jones, 2016). The decarbonization of the industrial heat sector and
487 improvement in the energy efficiency of the processes has the potential to reduce aluminium cradle to
488 gate impacts. An estimation of 31% reduction of energy use in alumina refining by 2050 is forecasted
489 (Kermeli *et al.*, 2015). The electrification of industry could also be a possible pathway to reduce

490 environmental impacts and improve productivity, but operating costs in general are much higher than
491 fossil fuel-based heating (Wei, McMillan and de la Rue du Can, 2019). Indirect electrification using
492 hydrogen produced by electrolysis as an energy carrier and feedstock can also play a key role in industry
493 decarbonization (Wei, McMillan and de la Rue du Can, 2019) but ambitious, targeted and near-term
494 action is needed to further overcome barriers and reduce costs of hydrogen deployment (IEA, 2019).
495 Future research should be addressed to quantify more precisely the future impact of alumina refining
496 and identify the appropriate lever of action to reduce the impacts.

497 In the scenario development, the adoption of inert anode technology shows the potential to reduce
498 environmental impacts of aluminium production only after 2050. The scenarios assume that inert anode
499 process will become available at a larger scale. In addition, we assumed that this process does not incur
500 an increase in energy intensity based on economic and competitiveness reasoning. The combination of
501 inert anode and wettable cathode seems to be a promising opportunity to achieve this goal (Haraldsson
502 and Johansson, 2018; Gupta and Basu, 2019) but those technologies are not commercialized yet.

503 The upscaling to total global emissions has been made using an exogenous aluminum demand
504 projection that is not influenced by the SSP narratives. Linking material consumption to SSPs framework
505 is relevant because material use has important consequences for environmental pressures and socio-
506 economic activities (Schandl *et al.*, 2020). On one hand, greener scenario could lead to a higher level of
507 dematerialization and material efficiency but on the other hand, aluminium can substitute other
508 materials and be used for novel applications leading to an increase of consumption. For example, due to
509 a substantial increase of aluminium in transport for light weighting vehicles, aluminium demand could
510 increase in sustainable scenarios. While future projections of material consumption are out of the scope
511 of this study, further research should explore the links between future demand, recycling dynamics and
512 regional market share to these narratives.

513 Despite the limitations, the prospective results generated by the PRISMAL framework provide significant
514 indications of environmental improvement potentials of the aluminium industry.

515 4.3 CONCLUSION

516 Prospective life cycle impacts of aluminum production sector were modelled up to 2050 and 2100 based
517 on the Share Socioeconomic Pathways. The narratives were leveraged to model technology penetration
518 and grid mix evolution. Results project a global average carbon intensity ranging between 8.6 and 18.0
519 kg CO₂ eq/kg in 2100 for baseline scenarios compared to 18.3 kg CO₂ eq/kg at present level. Further
520 reduction, under 5.0 kg CO₂ eq/kg, is realistic with aggressive policy efforts in the energy sector. The
521 evolution of other environmental indicators showed environmental co-benefits of a decarbonized
522 future. Changes in smelting technology (improvement of energy intensity and adoption of inert anode
523 process) are not enough to decouple GHG emissions to aluminium production. The impacts of the
524 electricity are the main lever for improvement.

525 The anchoring of this work in the SSP framework and results ensure consistency within scenario
526 modeling and within the scientific community. While, the study mainly focusses on the primary
527 production of the aluminium, future research could integrate PRISMAL results, the SSP narratives and
528 the stock dynamics of the whole aluminium value chain.

529

530 REFERENCES

- 531 Alcoa (2019) *Sustainability Report*.
- 532 Allwood, J. M. and Cullen, J. M. (2012) *Sustainable materials - With both eyes open*. Cambridge: UIT
533 Cambridge Ltd. Available at: <http://www.withbotheyesopen.com/pdftransponder.php?c=100> (Accessed:
534 27 August 2018).
- 535 Andrey S., Y., Sai Krishna, P. and Peter V., P. (2018) 'Progress of Inert Anodes in Aluminium Industry:
536 Review', *Journal of Siberian Federal University. Chemistry*, 11(1), pp. 18–30. doi: 10.17516/1998-2836-
537 0055.
- 538 Bangs, C. E. (2011) *Rolling Out Aluminium to Meet IPCC 2050 - A Dynamic MFA Approach for Greenhouse
539 Gas Emission Projections for the Aluminium Industry*. NTNU. doi: 10.13140/RG.2.2.19000.75527.
- 540 Bauer, N. *et al.* (2017) 'Shared Socio-Economic Pathways of the Energy Sector – Quantifying the
541 Narratives', *Global Environmental Change*, 42, pp. 316–330. doi: 10.1016/j.gloenvcha.2016.07.006.
- 542 Bertram, M. *et al.* (2017) 'A regionally-linked, dynamic material flow modelling tool for rolled, extruded
543 and cast aluminium products', *Resources, Conservation and Recycling*. Elsevier, 125, pp. 48–69. doi:
544 10.1016/J.RESCONREC.2017.05.014.
- 545 Bertram, M., Buxmann, K. and Furrer, P. (2009) 'Analysis of greenhouse gas emissions related to
546 aluminium transport applications', *International Journal of Life Cycle Assessment*. Springer, 14(SUPPL. 1),
547 pp. 62–69. doi: 10.1007/s11367-008-0058-0.
- 548 Bui, M. *et al.* (2018) 'Carbon capture and storage (CCS): The way forward', *Energy and Environmental
549 Science*. Royal Society of Chemistry, pp. 1062–1176. doi: 10.1039/c7ee02342a.
- 550 Bulle, C. *et al.* (2019) 'IMPACT World+: a globally regionalized life cycle impact assessment method', *The*

551 *International Journal of Life Cycle Assessment*. Springer Berlin Heidelberg, pp. 1–22. doi:
552 10.1007/s11367-019-01583-0.

553 Chen, W. Q. (2017) ‘Dynamic Product-Level Analysis of In-Use Aluminum Stocks in the United States’,
554 *Journal of Industrial Ecology*, 00(0), pp. 1–11. doi: 10.1111/jiec.12710.

555 Chen, X. and Önal, H. (2016) ‘Renewable energy policies and competition for biomass: Implications for
556 land use, food prices, and processing industry’, *Energy Policy*. Elsevier Ltd, 92, pp. 270–278. doi:
557 10.1016/j.enpol.2016.02.022.

558 Cullen, J. M. and Allwood, J. M. (2013) ‘Mapping the global flow of aluminum: From liquid aluminum to
559 end-use goods’, *Environmental Science and Technology*, 47(7), pp. 3057–3064. doi: 10.1021/es304256s.

560 Edenhofer, O. et al. (2014) *Climate Change 2014. Mitigation of Climate Change. Working Group III*
561 *Contribution to the Fifth Assessment Report of the Intergovernmental Panel on Climate Change*.
562 Cambridge, United Kingdom and New York, NY, USA.: Cambridge University Press.

563 Elysis (2020) *What is ELYSIS?* Available at: <https://www.elysis.com/en/what-is-elysis> (Accessed: 3
564 February 2020).

565 ELYSIS (2019) *Rio Tinto and Alcoa announce world’s first carbon-free aluminium smelting process*.
566 Available at: [https://www.elysis.com/en/rio-tinto-and-alcoa-announce-worlds-first-carbon-free-](https://www.elysis.com/en/rio-tinto-and-alcoa-announce-worlds-first-carbon-free-aluminium-smelting-process)
567 [aluminium-smelting-process](https://www.elysis.com/en/rio-tinto-and-alcoa-announce-worlds-first-carbon-free-aluminium-smelting-process) (Accessed: 9 January 2020).

568 Foster, R. N. (1986) *Innovation : the attacker’s advantage*. Summit Books.

569 Gibon, T., Arvesen, A. and Hertwich, E. G. (2017) ‘Life cycle assessment demonstrates environmental co-
570 benefits and trade-offs of low-carbon electricity supply options’, *Renewable and Sustainable Energy*
571 *Reviews*. Elsevier Ltd, pp. 1283–1290. doi: 10.1016/j.rser.2017.03.078.

572 Gupta, A. and Basu, B. (2019) 'Sustainable Primary Aluminium Production: Technology Status and Future
573 Opportunities', *Transactions of the Indian Institute of Metals*. Springer, 72(8), pp. 2135–2150. doi:
574 10.1007/s12666-019-01699-9.

575 Haraldsson, J. and Johansson, M. T. (2018) 'Review of measures for improved energy efficiency in
576 production-related processes in the aluminium industry – From electrolysis to recycling', *Renewable and
577 Sustainable Energy Reviews*. Elsevier Ltd, 93(May), pp. 525–548. doi: 10.1016/j.rser.2018.05.043.

578 Hatayama, H. *et al.* (2007) 'Dynamic Substance Flow Analysis of Aluminum and Its Alloying Elements',
579 *Materials Transactions*, 48(9), pp. 2518–2524. doi: 10.2320/matertrans.MRA2007102.

580 Hatayama, H. *et al.* (2012) 'Evolution of aluminum recycling initiated by the introduction of next-
581 generation vehicles and scrap sorting technology', *Resources, Conservation and Recycling*, 66, pp. 8–14.
582 doi: 10.1016/j.resconrec.2012.06.006.

583 Heidari, H. (2012) *Development of wettable cathode for aluminum smelting*. Université Laval. Available
584 at: <http://citeseerx.ist.psu.edu/viewdoc/download?doi=10.1.1.427.9477&rep=rep1&type=pdf>
585 (Accessed: 5 April 2019).

586 Hertwich, E. G. *et al.* (2015) 'Integrated life-cycle assessment of electricity-supply scenarios confirms
587 global environmental benefit of low-carbon technologies', *Proceedings of the National Academy of
588 Sciences of the United States of America*. National Academy of Sciences, 112(20), pp. 6277–6282. doi:
589 10.1073/pnas.1312753111.

590 Hydro (2020) *The world's most energy-efficient aluminium production technology*. Available at:
591 [https://www.hydro.com/en-US/about-hydro/stories-by-hydro/the-worlds-most-energy-efficient-
592 aluminium-production-technology/](https://www.hydro.com/en-US/about-hydro/stories-by-hydro/the-worlds-most-energy-efficient-aluminium-production-technology/) (Accessed: 5 February 2021).

593 IAI (2020a) *Global aluminium cycle*. Available at: <https://alucycle.world-aluminium.org/public-access/>

594 (Accessed: 13 October 2020).

595 IAI (2020b) *Mass Flow Statistics*. Available at: <http://www.world-aluminium.org/statistics/massflow/>

596 (Accessed: 1 May 2020).

597 IAI (2020c) *Primary Aluminium Production*. Available at: [http://www.world-](http://www.world-aluminium.org/statistics/#data)

598 [aluminium.org/statistics/#data](http://www.world-aluminium.org/statistics/#data) (Accessed: 6 February 2020).

599 IAI (2020d) *Primary Aluminium Smelting Energy Intensity*. Available at: [http://www.world-](http://www.world-aluminium.org/statistics/primary-aluminium-smelting-energy-intensity/)

600 [aluminium.org/statistics/primary-aluminium-smelting-energy-intensity/](http://www.world-aluminium.org/statistics/primary-aluminium-smelting-energy-intensity/) (Accessed: 25 February 2020).

601 IAI (2020e) *Primary Aluminium Smelting Power Consumption*. Available at: [http://www.world-](http://www.world-aluminium.org/statistics/primary-aluminium-smelting-power-consumption/)

602 [aluminium.org/statistics/primary-aluminium-smelting-power-consumption/](http://www.world-aluminium.org/statistics/primary-aluminium-smelting-power-consumption/) (Accessed: 2 March 2020).

603 IEA (2019) *The Future of Hydrogen – Seizing today’s opportunities*. Available at:

604 <https://www.iea.org/reports/the-future-of-hydrogen> (Accessed: 26 January 2021).

605 Kermeli, K. *et al.* (2015) ‘Energy efficiency improvement and GHG abatement in the global production of

606 primary aluminium’, *Energy Efficiency*. Springer Netherlands, 8(4), pp. 629–666. doi: 10.1007/s12053-

607 014-9301-7.

608 Koch, M. and Harnisch, J. (2002) ‘CO₂ emissions related to the electricity consumption in the European

609 primary aluminium production. A comparison of electricity supply approaches’, *International Journal of*

610 *Life Cycle Assessment*. Springer, 7(5), pp. 283–289. doi: 10.1007/BF02978889.

611 Kovács, V. B. and Kiss, L. (2015) ‘Comparative analysis of the environmental impacts of aluminium

612 smelting technologies’, in *Light Metals*. Cham: Springer International Publishing, pp. 529–534. doi:

613 10.1007/978-3-319-48248-4_88.

614 Kriegler, E. *et al.* (2014) ‘A new scenario framework for climate change research: the concept of shared

615 climate policy assumptions', *Climatic Change*. Springer Netherlands, 122(3), pp. 401–414. doi:
616 10.1007/s10584-013-0971-5.

617 Li, J. *et al.* (2008) 'Research progress in TiB₂ wettable cathode for aluminum reduction', *JOM*. Springer,
618 60(8), pp. 32–37. doi: 10.1007/s11837-008-0104-1.

619 Liu, G. and Müller, D. B. (2013) 'Centennial evolution of aluminum in-use stocks on our aluminized
620 planet', *Environmental Science and Technology*, 47(9), pp. 4882–4888. doi: 10.1021/es305108p.

621 Månberger, A. and Stenqvist, B. (2018) 'Global metal flows in the renewable energy transition: Exploring
622 the effects of substitutes, technological mix and development', *Energy Policy*. Elsevier Ltd, 119, pp. 226–
623 241. doi: 10.1016/j.enpol.2018.04.056.

624 Material Economics (2016) 'The Circular Economy - A powerful force for climate mitigation - Full Report',
625 pp. 1–7. doi: 10.1038/531435a.

626 Maung, K. N. *et al.* (2017) 'Assessment of secondary aluminum reserves of nations', *Resources*,
627 *Conservation and Recycling*. Elsevier, 126(February), pp. 34–41. doi: 10.1016/j.resconrec.2017.06.016.

628 Maurice Bödeker, J. and Bauer Martin Pehnt Heidelberg, M. (2010) *Aluminium and Renewable Energy*
629 *Systems-Prospects for the Sustainable Generation of Electricity and Heat Final version commissioned by*
630 *the International Aluminium Institute*.

631 McGeer, J. P. (1986) 'Hall-Heroult: 100 Years of Processes Evolution', *JOM*. Springer, 38(11), pp. 27–33.
632 doi: 10.1007/BF03257618.

633 McMillan, C. A. and Keoleian, G. A. (2009) 'Not All Primary Aluminum Is Created Equal: Life Cycle
634 Greenhouse Gas Emissions from 1990 to 2005', *Environmental Science & Technology*, 43(5), pp. 1571–
635 1577. doi: 10.1021/es800815w.

636 Moreau, V., Dos Reis, P. and Vuille, F. (2019) 'Enough Metals? Resource Constraints to Supply a Fully
637 Renewable Energy System', *Resources*. MDPI AG, 8(1), p. 29. doi: 10.3390/resources8010029.

638 Moss, R. H. *et al.* (2010) 'The next generation of scenarios for climate change research and assessment'.
639 doi: 10.1038/nature08823.

640 Müller, D. B., Liu, G. and Bangs, C. (2013) 'Stock Dynamics and Emission Pathways of the Global
641 Aluminum Cycle', *Nature Climate Change*. Nature Publishing Group, 2(10), p. 178. doi:
642 10.1002/9781118679401.ch46.

643 Nunez, P. and Jones, S. (2016) 'Cradle to gate: life cycle impact of primary aluminium production', *The
644 International Journal of Life Cycle Assessment*. The International Journal of Life Cycle Assessment,
645 21(11), pp. 1594–1604. doi: 10.1007/s11367-015-1003-7.

646 O'Neill, B. C. *et al.* (2017) 'The roads ahead: Narratives for shared socioeconomic pathways describing
647 world futures in the 21st century', *Global Environmental Change*. Pergamon, 42, pp. 169–180. doi:
648 10.1016/J.GLOENVCHA.2015.01.004.

649 Obaidat, M. *et al.* (2018) 'Energy and exergy analyses of different aluminum reduction technologies',
650 *Sustainability*, 10(4), pp. 1–21. doi: 10.3390/su10041216.

651 Paraskevas, D., Van de Voorde, A., *et al.* (2016) 'Current Status, Future Expectations and Mitigation
652 Potential Scenarios for China's Primary Aluminium Industry', *Procedia CIRP*. Elsevier, 48, pp. 295–300.
653 doi: 10.1016/J.PROCIR.2016.03.150.

654 Paraskevas, D., Kellens, K., *et al.* (2016) 'Environmental Impact Analysis of Primary Aluminium
655 Production at Country Level', *Procedia CIRP*. Elsevier, 40, pp. 209–213. doi:
656 10.1016/J.PROCIR.2016.01.104.

657 Pedneault, J. and Majeau-Bettez, G. (2021) 'PRISMAL Code'. doi:

658 <http://doi.org/10.5281/zenodo.4599725>.

659 Riahi, K. *et al.* (2017) 'The Shared Socioeconomic Pathways and their energy, land use, and greenhouse
660 gas emissions implications: An overview', *Global Environmental Change*. Pergamon, 42, pp. 153–168.
661 doi: 10.1016/J.GLOENVCHA.2016.05.009.

662 Rio Tinto (2019) *Our approach to climate change*.

663 Rogelj, J. *et al.* (2018) 'Scenarios towards limiting global mean temperature increase below 1.5 °c',
664 *Nature Climate Change*. Nature Publishing Group, 8(4), pp. 325–332. doi: 10.1038/s41558-018-0091-3.

665 Rombach, G., Modaresi, R. and Müller, D. B. (2012) 'Aluminium Recycling - Raw Material Supply from a
666 Volume and Quality Constraint System', *World of Metallurgy*, 65(3), pp. 157–162. Available at:
667 <https://www.researchgate.net/publication/257984464> (Accessed: 11 July 2018).

668 RUSAL (2018) *Sustainability report*.

669 RUSAL (2020) *RUSAL begins testing of new generation of inert anode pot*. Available at:
670 [https://rusal.ru/en/press-center/press-releases/rusal-begins-testing-of-new-generation-of-inert-anode-](https://rusal.ru/en/press-center/press-releases/rusal-begins-testing-of-new-generation-of-inert-anode-pot-/)
671 [pot-/](https://rusal.ru/en/press-center/press-releases/rusal-begins-testing-of-new-generation-of-inert-anode-pot-/) (Accessed: 7 July 2020).

672 Ryberg, D., Robinius, M. and Stolten, D. (2018) 'Evaluating Land Eligibility Constraints of Renewable
673 Energy Sources in Europe', *Energies*. MDPI AG, 11(5), p. 1246. doi: 10.3390/en11051246.

674 Saevarsdottir, G., Kvande, H. and Welch, B. J. (2020) 'Aluminum Production in the Times of Climate
675 Change: The Global Challenge to Reduce the Carbon Footprint and Prevent Carbon Leakage', *JOM*.
676 Springer, 72(1), pp. 296–308. doi: 10.1007/s11837-019-03918-6.

677 Schandl, H. *et al.* (2020) 'Shared socio-economic pathways and their implications for global materials
678 use', *Resources, Conservation and Recycling*. Elsevier B.V., 160, p. 104866. doi:

679 10.1016/j.resconrec.2020.104866.

680 Tian, Y. *et al.* (2013) 'Industry test of perforation anode in aluminium electrolysis technology', in
681 *Minerals, Metals and Materials Series*. Springer International Publishing, pp. 567–571. doi: 10.1007/978-
682 3-319-65136-1_97.

683 Vatne, H. E. (2019) 'TMS Light Metals Keynote Presents Realities of Aluminum's Environmental
684 Sustainability', *Ligth Metals Age*, (June).

685 Verones, F. *et al.* (2017) 'LCIA framework and cross-cutting issues guidance within the UNEP-SETAC Life
686 Cycle Initiative', *Journal of Cleaner Production*. Elsevier Ltd, 161, pp. 957–967. doi:
687 10.1016/j.jclepro.2017.05.206.

688 van Vuuren, Detlef P *et al.* (2011) 'The representative concentration pathways: an overview', *Climatic
689 Change*, 109, pp. 5–31. doi: 10.1007/s10584-011-0148-z.

690 Wei, M., McMillan, C. A. and de la Rue du Can, S. (2019) 'Electrification of Industry: Potential, Challenges
691 and Outlook', *Current Sustainable/Renewable Energy Reports*. Springer Science and Business Media LLC,
692 6(4), pp. 140–148. doi: 10.1007/s40518-019-00136-1.

693 Wernet, G. *et al.* (2016) 'The ecoinvent database version 3 (part I): overview and methodology', *The
694 International Journal of Life Cycle Assessment*, 21, pp. 1218–1230. doi: 10.1007/s11367-016-1087-8.

695 Worighi, I. *et al.* (2019) 'Integrating renewable energy in smart grid system: Architecture, virtualization
696 and analysis', *Sustainable Energy, Grids and Networks*. Elsevier Ltd, 18, p. 100226. doi:
697 10.1016/j.segan.2019.100226.

698

699